Vol 18 No 8, August 2009
1674-1056/2009/18(08)/3484-06

Chinese Physics B

© 2009 Chin. Phys. Soc.
and IOP Publishing Ltd

A numerical simulation of surface wave excitation in a rectangular planar-type plasma source*

Chen Zhao-Quan(陈兆权)†, Liu Ming-Hai(刘明海)‡, Lan Chao-Hui(蓝朝晖), Chen Wei(陈 伟), Tang Liang(唐 亮), Luo Zhi-Qing(罗志清), Yan Bao-Rong(燕保荣), Lü Jian-Hong(吕建红), and Hu Xi-Wei(胡希伟)

Key Laboratory of Fusion and Advanced Electromagnetic Technology of Ministry of Education, College of Electrical & Electronic Engineering, Huazhong University of Science and Technology, Wuhan 430074, *China*

(Received 20 September 2008; revised manuscript received 14 October 2008)

The principle of surface wave plasma discharge in a rectangular cavity is introduced simply based on surface plasmon polariton theory. The distribution of surface-wave electric field at the interface of the plasma-dielectric slab is investigated by using the three-dimensional finite-difference time-domain method (3D-FDTD) with different slot-antenna structures. And the experimental image of discharge with a novel slot antenna array and the simulation of the electric field with this slot antenna array are both displayed. Combined with the distribution of surface wave excitation and experimental results, the numerical simulation performed by using 3D-FDTD is shown to be a useful tool in the computer-aided antenna design for large area planar-type surface-wave plasma sources.

Keywords: surface wave plasma, numerical simulation, three-dimensional finite-difference time-domain method, surface plasmons polaritons

PACC: 5280P, 5265, 5240D

1. Introduction

A great deal of attention has been paid recently to surface wave plasma (SWP) extensively used for various potential applications in modern industry, such as ultra-large scale integration (ULSI) devices, liquid-crystal displays (LCD), solar cells and superficial modification of material. SWP has many merits in comparison with other types of plasma sources: (i) operation without the external magnetic field used in electron cyclotron resonance (ECR) or inductively coupled plasma (ICP); (ii) no impurity contamination caused from the electrode insertion in capacitive coupled plasma (CCP); (iii) high density plasma above the cut-off density with low pressure; (iv) with the small aperture antenna, the larger-area high-density planar surface wave plasmas can be realized through the surface-wave dissemination. Therefore, SWP has been exhaustively investigated both theoretically and experimentally.[1−9] For example, the significant effect of the antenna structure on the production of high density was reported in Ref.[1]; the influence of the incident microwave power, the gaseous component, the gas pressure and the shape of coupler antenna on the generation of plasma was investigated in Refs.[10]–[13]; the plasma wave resonance in the plasma guided by a vane-type slow wave structure was studied in Refs.[14] and [15].

To date, significant progress has been made in this field[1−15] and several SWP sources have already been used in the production of solar cell or liquid crystal panels. However, some problems, like the antenna-surface wave (SW) coupling mechanism and the optimum design of the slot antenna, have not been satisfactorily resolved yet. Chen *et al*[16] have analysed two-dimensional numerical simulations based on the finite-difference time-domain (FDTD) method in a cylinder planar-type non-magnetized plasma processing device. Kousaka and Ono[17] have performed numerical analysis by using the two-dimensional finite-difference time-domain method (2D-FDTD) in a microwave plasma source excited by azimuthally symmetric surface waves. Okamura *et al*[18] have simulated the TM_{01}-mode microwave propagation for plasmas with disk-plate windows by using the 2D-FDTD method.

*Project supported by the Foundation for Returned Scholars, the Ministry of Education of China.

†Corresponding author. E-mail: chenzhaoquan2007@smail.hust.edu.cn

‡E-mail: mhliu@mail.hust.edu.cn

In the present paper, we introduce the FDTD numerical method and try to investigate these problems with the aid of a computer. A three-dimensional model of the SWP source is built numerically based on the three-dimensional finite-difference time-domain method (3D-FDTD)[19] to study the electromagnetic fields in the system with different slot-antenna structures. In order to verify the credibility of this numerical simulation and to find the mechanism of the surface-wave discharge, the discharge experiment with a novel slot-antenna array[20] is also operated in a rectangular planar-type surface-wave plasma source.

2. Principle of surface wave plasma

In the experimental setup for the study of surface-wave plasma, the electromagnetic wave excited by slot-antennas accelerates the electrons and ionizes the low-pressure gas to form plasma. When the microwave power is high, the electromagnetic wave reflecting from the cut-off layer will disseminate along the interface of the dielectric board and plasma, thereby restricting its energy in the region near the interface, and decay exponentially with increasing propagation distance. Based on the theory of surface plasmon polaritons, the propagation constant k_{SP} on the planar dielectric-plasma interface is given by[1,12,20]

$$k_{SP} = k_0 \sqrt{\frac{\varepsilon_d \varepsilon_p}{\varepsilon_d + \varepsilon_p}}, \tag{1}$$

where k_0 is the vacuum wave vector and ε_p and ε_d are the relative permittivities for the metal and the dielectric, respectively. And ε_p is given as

$$\varepsilon_p = 1 - \frac{\omega_p^2}{\omega^2}, \tag{2}$$

where ω is the angular frequency of microwave and ω_p is the angular frequency of the plasma, expressed as

$$\omega_p = \left(e^2 n_e / \varepsilon_0 m_e\right)^{1/2}.$$

Figure 1 shows the configuration of the planar SWP source structure, which is the same as the configuration of the experimental setup under operation. The SWP source consists of an R22 rectangular waveguide connected to a metallic rectangular cavity 44 cm long, 20 cm wide and 30 cm high. The top wall of the cavity is of quartz dielectric with a thickness of 14 mm and relative permittivity $\varepsilon_d = 3.78$. The slot antenna in the figure can be replaced easily. The plasma reaches a high density (greater than the critical electron density at 2.45 GHz) by injecting microwave energy at 2.45 GHz from the waveguide into the cavity.

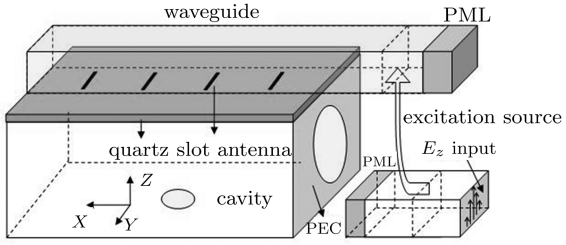


Fig.1. A three-dimensional model of the SWP source, where PML denotes the perfectly matched layer placed at the other end to avoid any reflection field in the 3D-FDTD code.

3. Numerical simulation using the 3D-FDTD code

3.1. The 3D-FDTD code based on Drude model

The cold non-magnetized electron plasma used in this work is assumed to have a fixed uniform electron density. The Maxwell's equations and plasma electron fluid equations are given by (Drude model)[21]

$$\begin{aligned}
\varepsilon \frac{\partial \boldsymbol{E}}{\partial t} &= \boldsymbol{\nabla} \times \boldsymbol{H} - \boldsymbol{J}, \\
\mu \frac{\partial \boldsymbol{H}}{\partial t} &= -\boldsymbol{\nabla} \times \boldsymbol{E}, \\
m_{\mathrm{e}} \frac{\partial \boldsymbol{u}}{\partial t} &= -e\boldsymbol{E} - \nu \boldsymbol{u}, \\
\boldsymbol{J} &= -e n_{\mathrm{e}} \boldsymbol{u},
\end{aligned} \tag{3}$$

where $\boldsymbol{E}$ and $\boldsymbol{H}$ are the electric and the magnetic fields, respectively, $\boldsymbol{J}$ is the current density in plasma, e is the electron charge, m_{e} is the mass of electron, n_{e} is the plasma electron density, ν is the electron-neutral collision frequency, $\boldsymbol{u}$ is the electron velocity, μ and ε are permeability and permittivity in free space or in quartz dielectric, respectively.

The 3D-FDTD method is employed to simulate surface wave excitation, and the 3D-FDTD code is edited in Fortran. The FDTD parameters are cell size $\Delta h = 2.5 \times 10^{-4}$ m and time step $\Delta t = 0.46 \times \Delta h/c$, where c is the speed of light. The Courant stability condition can be satisfied. The computational domain

including the waveguide and the cavity below is subdivided into 235 cells×110 cells×57 cells, and the calculations are carried out in at least 20000 time steps to obtain stable fields in the whole system. A 14 cells perfectly matched layer (PML) is designed to absorb the reflected waves. All conducting surfaces are approximated as lossless, perfect electrical conductors (PEC), while the plasma and the quartz are assumed to be homogeneous and isotropic. For the plasma parameters, the plasma electron density n_e and collision frequency ν can be set by the operator according to the actual experimental conditions.

3.2. Influence of the antenna structures

First of all we should know what sort of slot-antenna can stimulate the even stable surface electromagnetic wave. Therefore, the excitation of the antenna with three different longitudinal or transverse slot structures is simulated. Figure 2 depicts the schematic diagram of these metallic slot antennas. Figure 2(a) shows a single slot antenna lying along the x-direction, with 37.15 cm long and 1 cm wide; Figure 2(b) displays a 4-slot antenna located along the y-direction, where the slots are arranged along the x-direction and their interspaces are all 7.43 cm, and each slot is 5.6 cm long and 1 cm wide; Figure 2(c) shows a slot-antenna array with 10 longitudinal slots, each 3.6 cm long and 0.8 cm wide, and 4 transverse slots, each 5.6 cm long and 1 cm wide. Here, the plasma electron density n_e is assumed to be 2.25×10^{18} m^{-3} and the collision frequency ν is set as 3.0 GHz. The structure of the slot antenna is shifted as shown in Fig.2 in the simulation model, and the simulation results can be seen in Figs.3, 4 and 5.

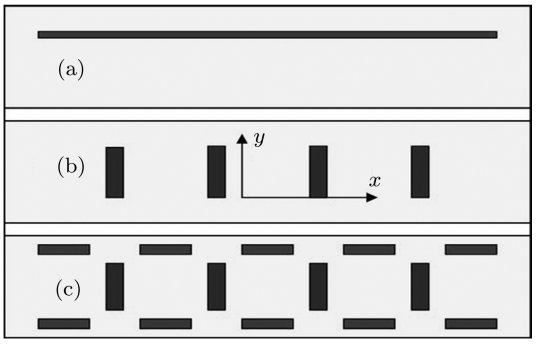


Fig.2. A schematic diagram of different metallic slot antennas: single longitudinal slot antenna (a); 4 transverse slots antenna (b) and a slot-antenna array with longitudinal slots and transverse slots (c).

Figure 3 shows the amplitude of the electric field excitation at the interface of the plasma-dielectric slab with the slot antenna shown in Fig.2(a). It can be found that even surface electric field distributed along the y-direction and the excitation in the x-direction are not well proportioned. Figure 4 displays the amplitude of the electric field excitation at the interface of the plasma-dielectric slab with the slot antenna shown in Fig.2(b). Even surface electric field distributed along the x-direction and the excitation in the y-direction are not obtained as shown in the figure.

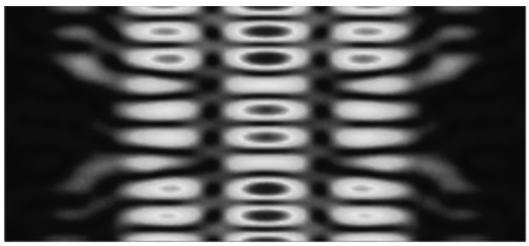


Fig.3. The amplitude of electric field excitation at the interface of the plasma-dielectric slab with the slot antenna shown in Fig.2(a).

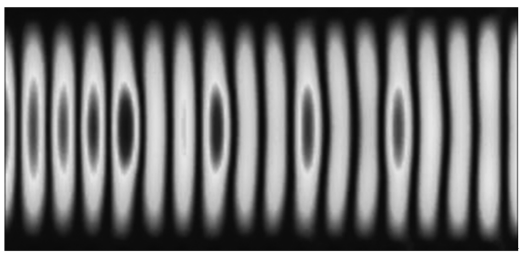


Fig.4. The amplitude of electric field excitation at the interface of the plasma-dielectric slab with the slot antenna shown in Fig.2(b).

Figure 5 shows the amplitude of the electric field excitation at the interface of the plasma-dielectric slab with the slot antenna shown in Fig.2(c). Compared with what is shown in Fig.4, the uniformity of the excitation is improved, but the surface electric fields in the y-direction are not found immediately in the figure, which do in fact exist. In comparing Fig.3 with Fig.4, we find that the relative peak value and the effective excitation area in Fig.4 are larger than those in Fig.3. Consequently, the excitation along the y-direction in Fig.5 has its distribution definitely, but its peak value is too small compared with the excitation of the transverse slots and cannot be displayed in the figure. Now we consider an actual discharge

process. When discharge starts, no larger area even plasma exists; if the distribution of the excitation is non-uniform, the uniformity of the discharge will be destroyed definitely and the occurrence of this situation in industrial applications will be disadvantageous. Therefore, although the peak value of the excitation in the y-direction is small, it is essential for the formation and the stability of the large area even surface-wave plasmas.



Fig.5. The amplitude of the electric field excitation at the interface of the plasma-dielectric slab with the slot antenna shown in Fig.2(c).

3.3. A comparison with experiment

In order to check the performance of the new antenna, we have made an aluminum slot-antenna array with the structure shown in Fig.2(c) and performed an experiment on our surface-wave plasma system.[20] Figure 6 shows the image of the discharge under the following condition: the input microwave power of 600 W, argon gas pressure of 100 Pa and the frequency of the microwave of 2.45 GHz. Five bright discharge areas along the x-direction and seven bright discharge areas along the y-direction can be found, separately. In Ref.[20], the electron temperature T_{e} was estimated to be 2.5 eV, i.e. $T_{\mathrm{e}} \approx 2.5$ eV and the electron density n_{e} was measured by using a Langmuir probe to be 8.1×10^{17} m^{-3}, i.e. $n_{\mathrm{e}} \approx 8.1\times10^{17}$ m^{-3}, and the uniform plasma within 14 cm with a fluctuation level of 5.5% was achieved. We can infer the collision frequency $\nu \approx$2.4 GHz (at a 100 Pa gas pressure) and adopt this parameter to simulate the excitation at the interface of the plasma-dielectric slab as shown in Fig.7. Unfortunately, the excitation peak number only in the y-direction can be compatible with the discharge image, for which the reason is that this discrepancy is caused possibly by the inaccurate value of the electron density obtained from the probe measurements. When we assume that the electron density $n_e = 1.1 \times 10^{18}$ m^{-3} and the collision frequency $\nu = 2.4$ GHz in our 3D-FDTD model, we can obtain a simulation result identical with the discharge image as shown in Fig.8.



Fig.6. The discharge image under the condition: microwave power of 600 W and argon gas pressure of 100 Pa.

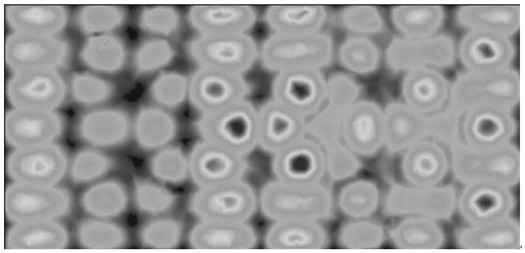


Fig.7. The excitation of the electric field at the interface of plasma-dielectric slab under the parameter condition: the electron density $n_e = 8.1 \times 10^{17}$ m^{-3} and the collision frequency $\nu = 2.4$ GHz.

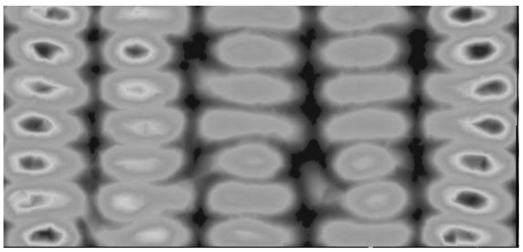


Fig.8. The excitation of the electric field at the interface of the plasma-dielectric slab under parameter condition: the electron density $n_e = 1.1 \times 10^{18}$ m^{-3} and the collision frequency $\nu = 2.4$ GHz.

3.4. The computation of energy flow

The computation of energy flow is one of the important items in the 3D simulation of the SWP source, and it can show the energy absorbed by the plasma. The energy flow S is calculated by[22−24]

$$S = \int (\boldsymbol{E} \times \boldsymbol{H}) \cdot \mathrm{d}\boldsymbol{A}, \tag{4}$$

where $\boldsymbol{E}$ and $\boldsymbol{H}$ are the electric and the magnetic fields in the waveguide, respectively, and d$\boldsymbol{A}$ is the area unit selected in the waveguide.

The SW propagates along the x-direction which is perpendicular to the direction of opening the slots. This is practically significant to the optimization of the antenna design which has to meet the challenge of increasing the absorbed energy by plasma as much as possible, with a simple and stable SW mode maintained at the same time. Figure 9 presents the energy flow versus time step with the antenna shown in Fig.2(c).[19] The sampling plane is placed at 5 cells in front of the PML. We prescribe that the energy flow along the x-direction is positive, thus the energy flow shown in Fig.9 is negative. The time step number is limited to 1400, so the electromagnetic fields in the system are far from being stable. However, we can also roughly see the proportion of energy absorbed by the plasma. The calculations of energy flow or reflection power provide us with a tool to compare the radiation efficiencies of different slot antennas.

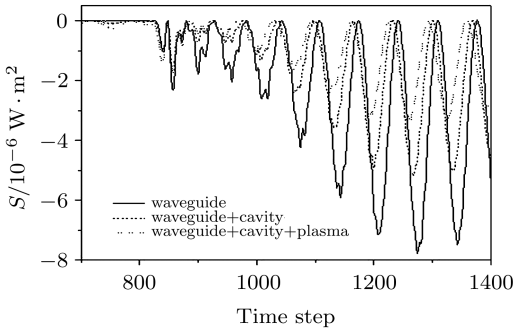


Fig.9. Energy flow versus time step, where the sampling plane is located at 5 cells in front of PML.

3.5. Result analysis

Generally, in our experimental setup for the study of surface-wave plasma, firstly, the electromagnetic wave excited by slot-antennas enters into the vacuum cavity, thereby forming the distribution of the electromagnetic wave and accelerating electrons to ionize the low-pressure Ar gas into the plasma. Secondly, with plasma density increasing, the electromagnetic wave will be reflected from the cut-off layer and will disseminate along the interface between the dielectric board and plasma, thereby restricting its energy in the region near the interface, and decays exponentially with propagation distance increasing. And then the electromagnetic surface-wave and surface plasmon polaritons are formed at the dielectric-plasma interface as shown in Fig.4. Finally, the electrons accelerated by the surface-wave electrical field collide with the neutral Ar atoms and so the density of the Ar excited state atoms increases simultaneously. When a large number of particles in a higher energy Ar excited state turn into particles in a lower energy state, we can observe the bright image of this discharge, as shown in Fig.6.

4. Conclusion

The theory of surface-wave plasma is recalled simply at first. The numerical simulation code 3D-FDTD is introduced to simulate the electromagnetic waves in a surface-wave plasma system, and the amplitudes of the electric field excitation at the interface of the plasma-dielectric slab are numerically displayed with different structure slot antennas. A microwave discharge experiment is operated by using the novel slot-antenna array. According to the plasma parameters obtained from experimental measurements, the results of the numerical simulation are compatible with theory and experiment. It is found that numerical simulation using the 3D-FDTD is a useful tool in the computer-aided antenna design for large area planar-type surface-wave plasma sources.

References

[1] Sugai H, Ghanashev I and Nagatsu M 1998 *Plasma Sources Sci. Technol.* **7** 192

[2] Nagatsu M, Naito K, Ogino A and Nanko S 2006 *Plasma Sources Sci. Technol.* **15** 37

[3] Ghanashev I and Sugai H 2000 *Physics of Plasmas* **7** 3051

[4] Liu P K and Xie H Q 2007 *Chin. Phys.* **16** 766

[5] Nagatsu M, Morita S, Ghanashev I, Ito A, Toyoda N and Sugai H 2000 *J. Phys.* D: *Appl. Phys.* **33** 1143

[6] Kousaka H, Ono K, Umehara N, Sawada I and Ishibashi K 2006 *Thin Solid Films* **506∼507** 503

[7] Huang W H, Liu G Z, Liu J Y, Ning H, Song X X and Zhou J S 2000 *Chin. Phys.* **9** 757

[8] Ghanashev I, Nagatsu M and Sugai H 1997 *Jpn. J. Appl. Phys.* **36** 337

[9] Liu M H, Sugai H, Hu X W, Ishijima T, Jiang Z H, Li B and Dan M 2006 *Acta Phys. Sin.* **55** 5905 (in Chinese)

[10] Wu C F, Zhan R J, Wen X H and Huang W D 2001 *IEEE Trans. Plas. Sci.* **29** 13

[11] Xu X, Liu F, Zhou Q H, Liang B, Liang Y Z and Liang R Q 2008 *Appl. Phys. Lett.* **92** 011501

[12] Liang Y Z, Ou Q R, Liang B and Liang R Q 2008 *Chin. Phys. Lett.* **25** 1761

[13] Liang B, Liang R Q, Liang Y Z and Ou Q R 2007 *Chin. Phys.* **16** 3732

[14] Wu T J and Kou C S 2005 *Physics of Plasmas* **12** 103504

[15] Wu T J, Guan W J, Tsai C M, Yeh W Y and Kou C S 2001 *Physics of Plasmas* **8** 3195

[16] Chen Q, Paul H A and Makoto K 1999 *IEEE Trans. Plas. Sci.* **27** 164

[17] Hiroyuki Kousaka and Kouichi Ono 2002 *Jpn. J. Appl. Phys.* **41** 2199

[18] Yoshimasa O, Yoshito Y, Kazuhiro F, Taiki M, Koji T, Hideki K, Shin K and Masakazu F 2007 *J. Vac. Sci. Technol.* **25** 816

[19] Lan C H, Chen Z Q, Liu M H and Hu X W 2009 *Plasma Sci. & Technol.* **11** 66

[20] Chen Z Q, Liu M H, Zhou P Q, Chen W, Lan C H and Hu X W 2008 *Plasma Sci. & Technol.* **10** 655

[21] Muller R, Malyarchuk V and Lienau C 2003 *Phys. Rev.* B **68** 205415

[22] Chen R S, Yang Y, Yang H W and Yuan H 2007 *Acta Phys. Sin.* **56** 1443 (in Chinese)

[23] Chen R S, Yang H W and Zhang Y 2006 *Acta Phys. Sin.* **55** 3464 (in Chinese)

[24] Cao J X, Song F L and Wang K 2005 *Acta Phys. Sin.* **54** 807 (in Chinese)